Multi-azimuth seismic imaging applied to naturally fractured and karstified reservoirs

Mitchel Xavier*[1], Marcio Spinola[1] and Luiz Eduardo Santos[2], [1]Halliburton, [2]Petrobras

This paper was prepared for presentation during the 18th International Congress of the Brazilian Geophysical Society held in Rio de Janeiro, Brazil, 16-19 October 2023.

Abstract

Multi-azimuth seismic data has been providing much better conditions for the success of petroleum exploration and reservoir characterization. The analysis of very complex geological areas become a less difficult task when seismic data from several different acquisition directions are available. This work presents a multi-azimuth synthetic seismic simulation applied to an area which represents a naturally fractured and karstified reservoir. Tridimensional acoustic modeling was used to simulate a multi-azimuth acquisition, with eight different azimuths, and to generate the seismic data. The Reverse Time Migration methodology was employed to conduct depth imaging of the data. Subsequently, a seismic volume was generated for each azimuth value. Lastly, a comparison was conducted among the eight seismic volumes to identify any discrepancies in the imaging results and to assess the extent to which these outcomes complement each other in terms of identifying geological karst features.

Introduction

In recent years, the option of performing more complex seismic data acquisitions has become increasingly common, such as multi-azimuth, wide-azimuth, OBN and OBC-type acquisitions, for example. The complexity is not only in the logistics, planning and execution of the data acquisition, but also in the processing of the acquired seismic data. On the other hand, these more complex data acquisitions, consequently, generate a greater amount of information, which facilitates the attempt to obtain a more reliable and accurate image of the subsurface structures, in the seismic processing and depth imaging stages.

Thus, one of the main advantages of multi-azimuth seismic acquisitions, if compared to the traditional narrow-azimuth acquisition (Figure 1), is the fact that it provides a better illumination of subsurface targets (LONG et al, 2006). In other words, in multi-azimuth acquisitions, a greater amount of energy reaches the subsurface and, consequently, a greater amount of energy returns to be registered in the receivers.

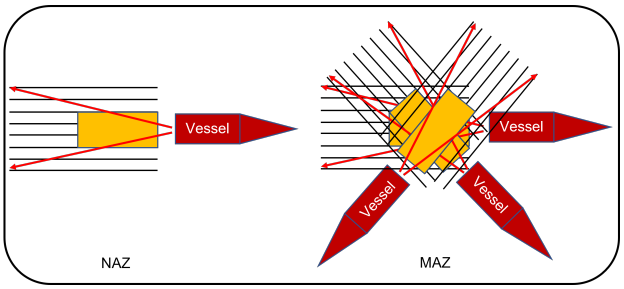

Figure 1: *Basic scheme of different seismic acquisition geometries: narrow (left) and multi-azimuth (right). The orange rectangle represents the illumination region. Based on LONG et al (2006).*

The imaging of carbonate bodies and certain structures that presents karstification, highly fractured regions and areas with occurrence of caves, for example, have been prominent themes within the scientific community linked to the oil industry. The correct identification of these features for a reliable and accurate mapping are of great importance both for the definition of exploratory wells and for the development, contributing to the success of drilling and characterization of reservoirs.

In terms of depth imaging, a series of works have been using techniques such as full waveform inversion (FWI), reverse time migration (RTM), least squares migration (LSM), seismic tomography, among others, to try to solve such challenges related to the image quality. LOH et al (2016), for example, demonstrated that with the use of a workflow involving anisotropic FWI, together with seismic tomography and application of a correction for Q absorption factor, it is possible to obtain better quality results in the imaging of karstified carbonates, when compared to isotropic FWI workflow results. SUN et al (2013) and TREADGOLD et al (2008) proposed anisotropic full azimuth imaging workflows, with amplitude preservation and analysis of seismic attributes, to obtain more reliable imaging and, consequently, greater accuracy in fracture detection.

This work aims to compare and analyze the results of a multi-azimuth seismic acquisition simulation applied to a geological region with naturally fractured and karstified reservoir (Figure 2), represented by a velocity model. Depth imaging was applied to the generated synthetic seismic data and then the seismic volumes were created. After that, the comparison among all seismic volumes was performed. Varied perspectives, such as depth slice, were used to help in the difference's identification.

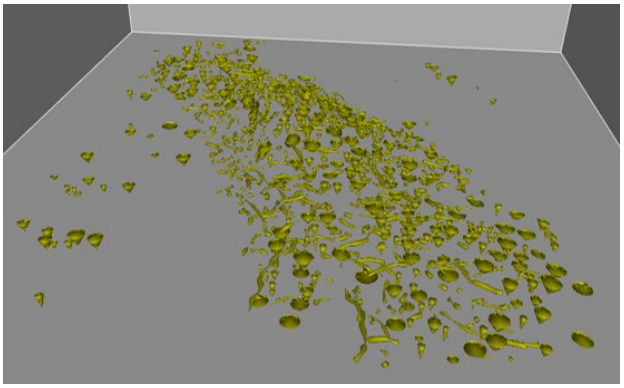

Figure 2: *Structural model based on a fractured and karstified geologic features. It was one of the inputs for the velocity model.*

Method

The first step was to get a velocity model with complex geological features and structures that simulates a naturally fractured and karstified reservoir (Figure 3). This was done using the results of a collaboration research tool able to model and simulate karst features.

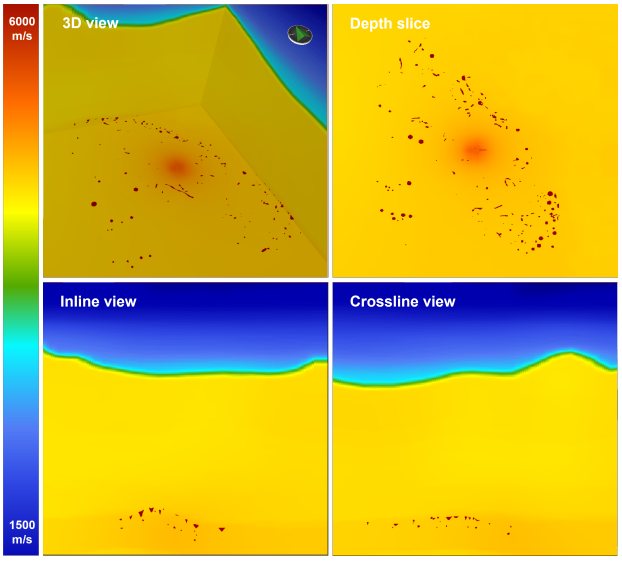

Figure 3: *Velocity model with complex structures. In the top, a tridimensional (left) and depth slice (right) views. In the bottom, Inline (left) and crossline (right) views.*

Next step was to perform the multi-azimuth seismic acquisition simulation. For that, based on the finite difference method (SMITH, 1985), a 3D acoustic seismic modeling was carried out. From the azimuth defined as 0° (Figure 4), the seismic acquisition configuration was rotated in the clockwise direction and at each value of 45° a new simulation was performed, until a complete turn was reached. Therefore, in addition to the 0° azimuth, seismic simulations were carried out for the azimuths of 45°, 90°, 135°, 180°, 225°, 270° and 315°. In Figure 4, it is possible to visualize on a map the seismic acquisition simulation configuration positioned at all the mentioned azimuth values, overlaying a depth slice of the velocity model. The maximum frequency for the acoustic seismic modeling was 45 Hz and the streamer length was 6 km.

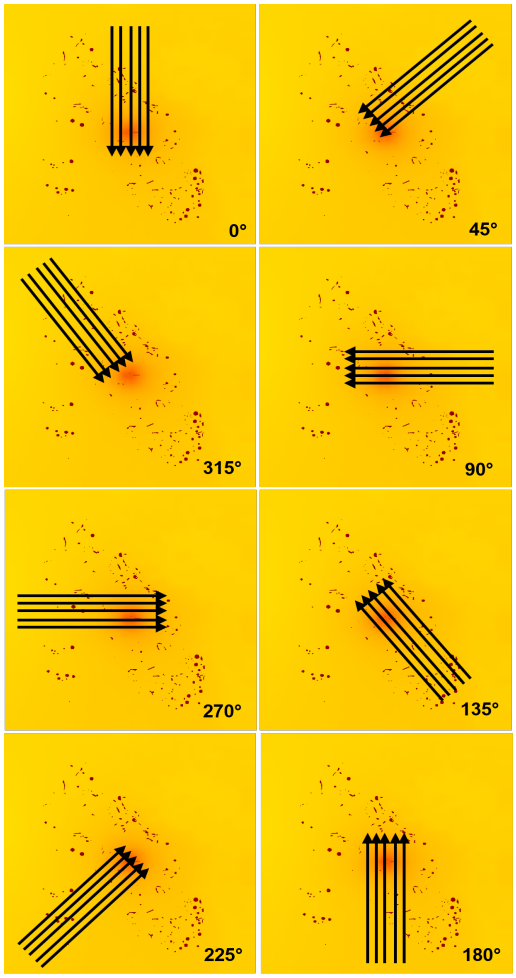

Figure 4: *Diagram of the eight azimuths values used for the seismic acquisition simulations, with a depth slice of the velocity model in the background.*

After carrying out the seismic acquisition simulation for all azimuth values mentioned and, therefore, generating synthetic seismic data for each of them, the next step was to perform the depth imaging process to all this generated data and, thus, obtain the seismic volumes. The chosen technique used to perform the depth imaging was the reverse time migration, also known as RTM migration (BAYSAL et al, 1983; WHITMORE, 1983; LEVIN, 1984). Basically, RTM Migration, using the full-wave equation, extrapolates the source wavefield forward and the receiver wavefield backward in time. Snapshots at each time step were calculated. The imaging condition known as excitation time is applied to produce a volume of depth imaging by convolution of the source and receiver wavefields at all times. The maximum frequency for RTM migration for this work was set to 45 Hz.

Results

In Figure 5, it is possible to see a bidimensional view of all generated seismic volumes. It is important to mention that the data didn't receive any treatment after migration, i.e., no post processing was applied. In the shallower area, for example, it is possible to see some problems as migration artifacts and coverage issues. But the goal of this study was concentrated in the imaging of the deeper part of the model, where complex structures, related to a naturally fractured and karstified reservoir, are situated. The identification of such structures is relatively easy in all seismic volumes, i.e., in all azimuths. For a better interpretation and comparison, a zoom was applied to the area of interest (Figure 6).

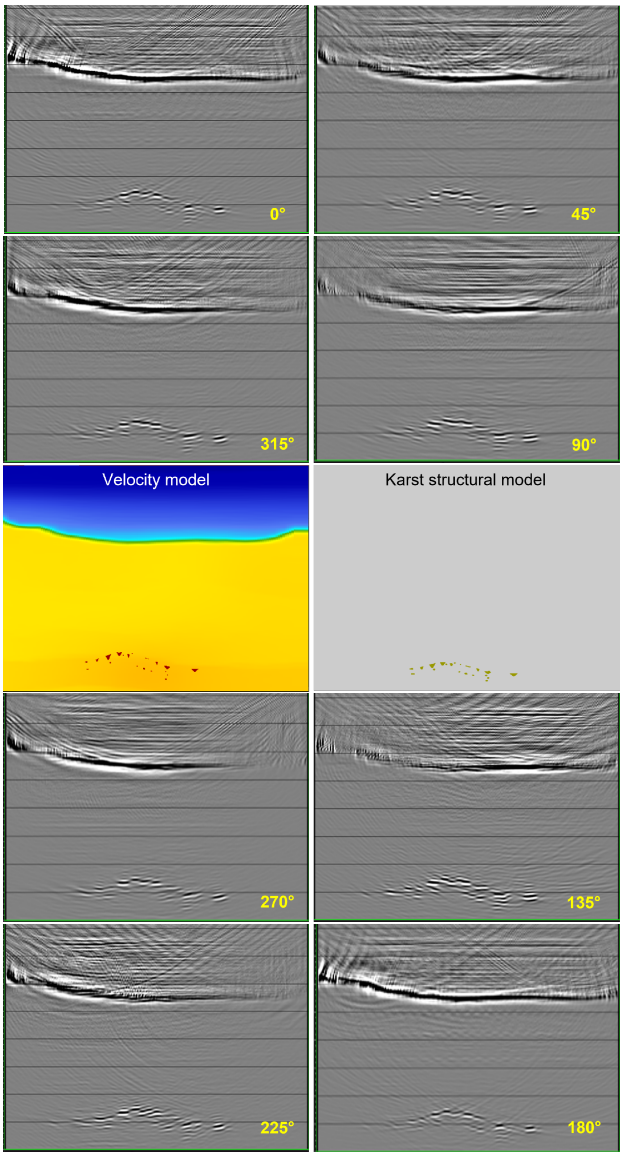

Figure 5: *Inline view of the seismic volumes, one for each azimuth value. In the middle of the figure, are the velocity model (left) and the structural model (right).*

In Figure 6, it is possible to see clear differences in the depth imaging results. When comparing the seismic volumes among each other and when comparing to the velocity and structural models, it is possible to better identify a certain region of the complex structure depending on the azimuth value. For example, the part of the structure located farthest to the right has a worse identification in the azimuths equal to 0° and 180° if compared to the others. In the other hand, the very tiny part of the structure located farthest to the left is much better identified in the azimuth equal to 135° and it is almost impossible to identify in some of the other azimuths. Regarding the very top of the structure, its shape is better represented in the azimuths equal to 90° and 270°.

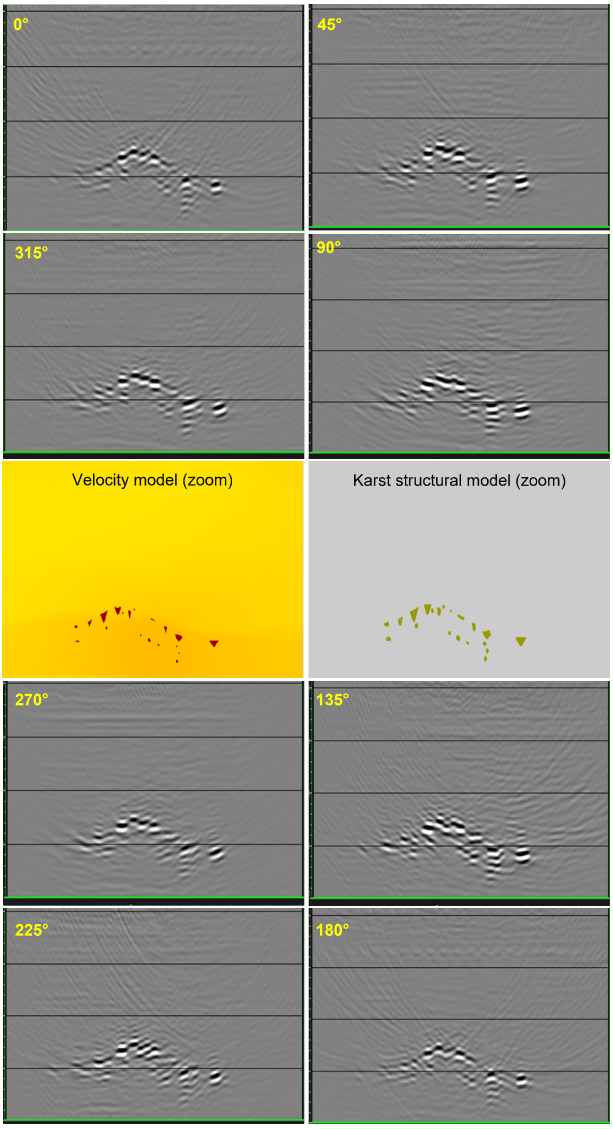

Figure 6: *Inline view. A close was applied to all seismic volumes in the region of the karstified structures. Again, in the middle of the figure, to support the analysis and comparison, are the velocity model (left) and in the structural model (right).*

In Figure 7, presents depth slices with same depth for each azimuth. In a reservoir characterization process, for example, the analysis, interpretation and quality control should be done in several different depths but the intention here is to show that the features related to the complex karstified features can be identified in all azimuths. Again, the differences in the seismic volumes are relatively easy to be seen.

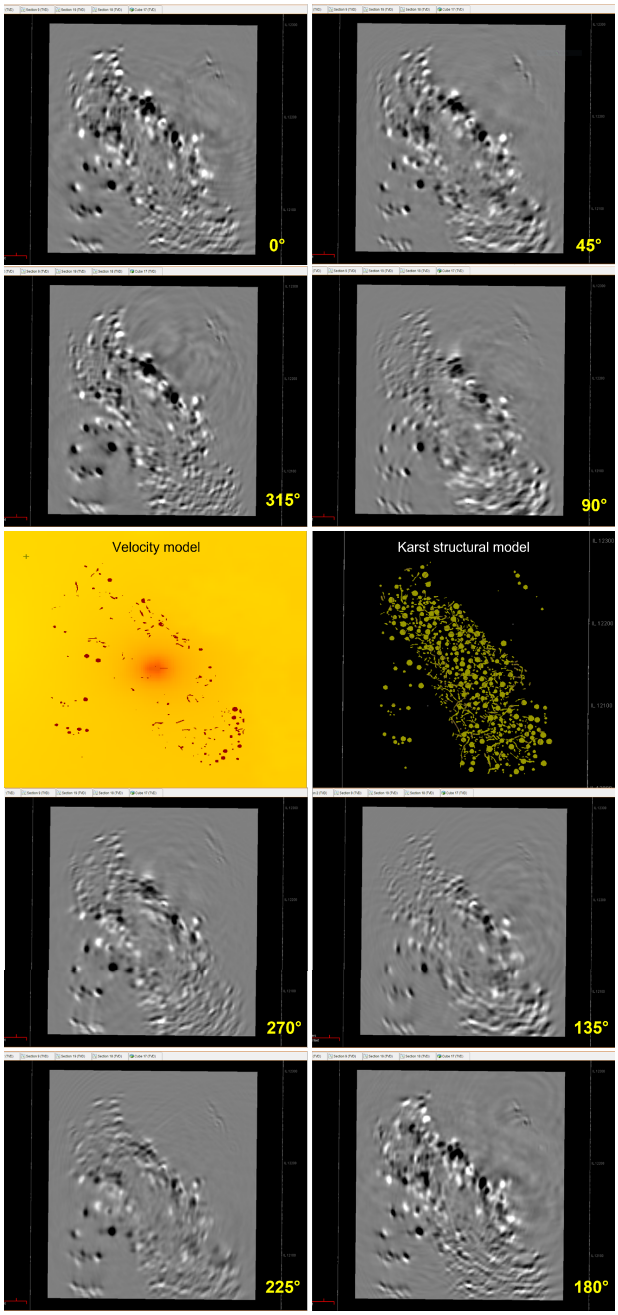

Figure 7: *Depth slice views. It is possible to clearly see some differences in the depth imaging results.*

Depending on the acquisition azimuth direction, it is very clear that the shape of certain karst features was affected by the direction. For example, the karst features in the lower left in the azimuth equal to 135°. Features in the upper left are more visible and identifiable in azimuths equal to 0°, 45°, 180° and 315° than in the others.

Another import way of use all the azimuths volumes is to sum all of them up and, thus, to create a new seismic volume. This operation was performed, and the result was used to try to identify three aleatory features associated with caves (Figures 8 and 9).

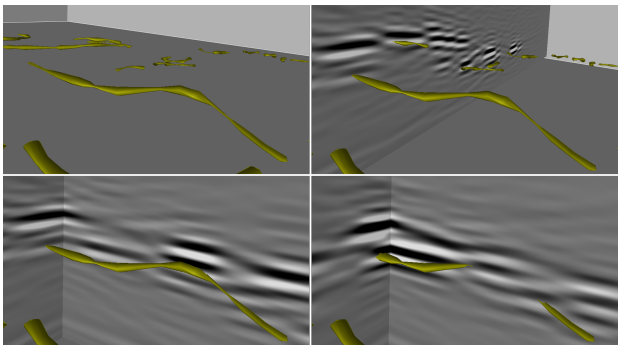

Figure 8: *Attempt to identify an arbitrary cave in the seismic volume. In the top left is the chosen cave. In the top right is the analysis of an inline. In the bottom left and right are the analysis of two different pairs of inlines and crosslines.*

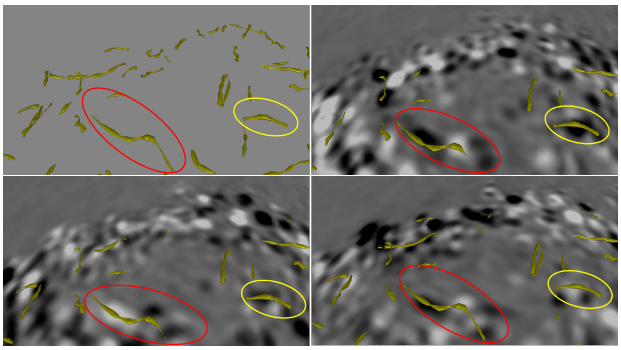

Figure 9: *Another attempt to identify arbitrary caves in the seismic volume were done using depth slices. In the top left are the chosen caves are highlighted. In the top right, in the bottom left and right three different depth slices are shown to facilitate the recognition of karst features in the seismic volume.*

In Figure 8 it is possible to see the seismic response related to the cave. Also, in In Figure 9, it is relatively clear that the chosen caves can be identified in the depth slice, including some variation in amplitude with direction which may be due to their complex shapes.

Conclusions

Multi-azimuth seismic acquisition, despite of its higher cost if compared to the traditional narrow azimuth acquisition, has been increasingly used in the last years. Petroleum companies realized that the benefits brought by the multi-azimuth results compensates by far the cost spent in the seismic acquisition campaign. When the geology of the subsurface is very complex, the more data available the more will be the chances to achieve good results during the reservoir characterization phase. This work presented a multi-azimuth seismic simulation applied to a complex geological region. After seismic modeling and depth imaging, eight seismic volumes were generated. In all seismic volumes, it was possible to identify with relative ease the simulate karst features. Often, it was easier to identify some structures in a specific azimuth when compared to another, which proves once again the idea that the direction in which the seismic acquisition is carried out directly influences the quality of the image result.

Acknowledgments

The authors would like to thank to ANP, Petrobras, and Halliburton for support during this work as well as our colleagues Carlos Seabra, Erwan Renaut and specially, we would like to thank posthumously our colleague Caroline Cazarin for all her contribution, encouragement, and inspiring example.

References

BAYSAL, E.; KOSLOFF, D.; SHERWOOD, J. W. C. 1983. Reverse Time Migration. Geophysics, V. 48, 1514-1524.

LEVIN, S. 1984. Principle of reverse-time migration. Geophysics, v.49, 581-583.

LOH, F. C.; CHUAH, B. L.; ZHOU, J.; MANNING, T.; WOLFARTH, S. e PRIYAMBODO, D. 2016. Subsea karst detection and imaging improvement using full waveform inversion. 78th EAGE Conference and Exhibition.

LONG, A. S.; PRAMIK, W.; FROMYR, E.; LAURAIN, R.; Chris PAGE. 2006. Multi-Azimuth and Wide-Azimuth lessons for better seismic imaging in complex settings, ASEG Extended Abstracts, 2006:1, 1-5.

SMITH, G.D. 1985. Numerical Solution of Partial Differential Equations (Finite Difference Methods). 3rd Edition, Oxford University Press, Oxford.

SUN, S. Z.; WANG, D. AND ZHOU, X. 2013. 3D amplitude-preserved full-azimuth anisotropic imaging and CRP gathering: An appealing method for integrated fracture detection. 83rd SEG Annual Meeting, Expanded Abstracts, 4071-4075.

TREADGOLD, G.; SICKING, C.; SUBLETTE, V. e HOOVER, G. 2008. Azimuthal processing for fracture prediction and image improvement. CSEG Recorder, 38–42.

WHITMORE, N. D. 1983. Iterative depth migration by backward time propagation. Expanded Abstracts, SEG-Society of Exploration Geophysicists.